Natural Resources Conservation and Research 2025, 8(1), 10187.
https://doi.org/10.24294/nrcr10187

Article

Climate change and its implication in the process of assessing the specific vulnerability of water resources in the intertropical zone

Franck Fabrice MBA[1,*], Henri Grisseur Djoukeng[1], Roger Ntankouo Njila[1], Mike Castane Makaya Mvoubou[2], Emile Temgoua[1]

[1] Department of Rural Engineering, Faculty of Agronomy and Agricultural Sciences, University of Dschang, Dschang 222, Cameroon
[2] Department of Geology, Faculty of Science, University of Sciences and Technology of Masuku, Franceville 901, Gabon
*** Corresponding author:** Franck Fabrice MBA, franckfabricemba@yahoo.fr

CITATION

MBA FF, Djoukeng HG, Njila RN, et al. Climate change and its implication in the process of assessing the specific vulnerability of water resources in the intertropical zone. Natural Resources Conservation and Research. 2025; 8(1): 10187. https://doi.org/10.24294/nrcr10187

ARTICLE INFO

Received: 8 November 2024
Accepted: 19 February 2025
Available online: 15 April 2025

Abstract: Economic activities in the humid intertropical zone are highly dependent on climate. The aim of this study is to identify the new sowing calendar period, then assess and map climate vulnerability, while tracing the potential impact of people's ability to adapt on the quality of water resources. Climate vulnerability is assessed by means of an exposure analysis based on 45 years of climate data (1976 to 2020) for the calculation of climate trends and standard anomalies, sensitivity, potential impact assessed following field surveys, and adaptive capacity. A multi-criterion analysis was used to map the level of vulnerability. The results show that climate change is gradual and has created a shift in the agricultural calendar, with the sowing period due to the return of the rains moving from early March to the second third of the same month. Agropastoral activities, water resources and people's health are all affected. Adaptation measures result in the production of waste that causes pollution. Pollutants may be physical, chemical, or microbiological in nature. Socio-economic development necessarily requires adaptations specific to the African context.

Keywords: agriculture; climate change; water management; human health; intertropical zone

1. Introduction

The African continent is one of the world's most vulnerable regions to climate change, due to the low adaptive capacity of its populations and widespread poverty [1]. In 2006, the United Nations Framework Convention on Climate Change proposed two strategies for dealing with global climate change: Mitigation and adaptation. Mitigation aims to limit climate change by reducing greenhouse gas emissions, while adaptation aims to alleviate adverse impacts through a wide range of actions on specific systems. The countries of Central Africa are classified as developing countries. The economy of this zone is climate-dependent, being essentially linked to climate-dependent activities such as agriculture and livestock farming. According to statistics provided by the African Development Bank in 2018, agriculture and breeding occupy 58% to 60% of the rural population and contribute between 25% and 40% of Gross Domestic Product [2,3]. In addition, climate change is having a negative impact on the availability of water resources and the drinking water and sanitation services that are essential for human health [4–6]. Given that farming and breeding activities, drinking water supply management systems, and sanitation services are highly dependent on the climate, good water management in the face of climate variability remains a major challenge for the countries of the sub-region, which very often pay little attention to it [7,8]. This is more imperative given that the population of most developing countries is estimated at 2,634,200,000 in cities [9]. Exponential population growth calls for high consumption of natural resources, some of which are non-renewable. The availability of a clean water supply is essential for human survival and various socio-economic purposes [10].

There are many studies on climate change. Modeling projections are indicative and not absolute [11]. Recent models are more sophisticated and show rapid changes in global temperatures and their impact on human society [12,13]. This is the case of the CMIP6 model for the assessment of climate variations through the production of future climate change scenarios while including runoff stimulation at different geographical scales [14,15]. Despite the various advances in climate models, the future impact of climate change remains subject to uncertainties and is still subject to systematic errors [16].

The issue of climate variability, which can lead to climate change, must therefore be a central concern for governments, especially in terms of adaptation given its dynamic nature [7,17], as the collection and processing of hydrological and hydrogeological data is not yet a major concern for most developing countries due to high costs and the lack of qualified personnel. In addition, changes in climate have a direct impact on socio-economic activities and the health of populations. Flashing back to the situation on the continent, according to [18], the coverage rate in urban areas in Africa passed from 77% in 1990 to 92% in 2008, which is expressed by the increase in the population served from 3.8 million to almost 10.0 million. Still in 2008, only 25% of the urban population was served by a private connection, a proportion comparable to that in 1990. In rural areas, the coverage rate passed from 31% to 51% between 1990 and 2008 [19]. The situation is similar in Cameroon, where, according to a 2016 report by the "Institut National de la Statistique" (INS), the coverage rate for access to drinking water was almost 61% in 2014, and for sanitation, 40%. The average rate of access to drinking water in Cameroon from 2018 was 77% of the population in urban areas and 45% in rural areas, according to the [20]. Despite the efforts made to date, there is still a shortage, as many of the Drinking Water Supply and Sanitation projects undertaken by decentralized local authorities are not operational as soon as they are built [21]. As a result, people rely on rainwater, streams, springs, and boreholes for their water, which unfortunately is not always of assured quality [19]. Particular attention is therefore paid to the influence of climatic variations on live systems and the implications for future research into specific water pollutants, especially in the current context of this study, which is marked by the absence of a conventional drinking water network. The present study therefore focuses on describing the meteorological data collected to correct the climatic data provided by the sensors in order to detect the influence of climatic variations on the agricultural calendar. More specifically, to identify the new sowing calendar period and then assess the influence of climate on live systems, the ability of populations to adapt, and the potential impact on the quality of water resources. This would make it easier to identify the specific pollutants to be used in a study to assess the specific vulnerability of water resources. Such a study will help to improve the living conditions of populations in the face of changing climatic conditions.

2. Materials and methods

2.1. Location of study area

The Department of Menoua is located in the West Cameroon Region, between latitudes 5°10′ N and 5°40′ N and between longitudes 9°50′ E and 10°20′ E (**Figure 1**).

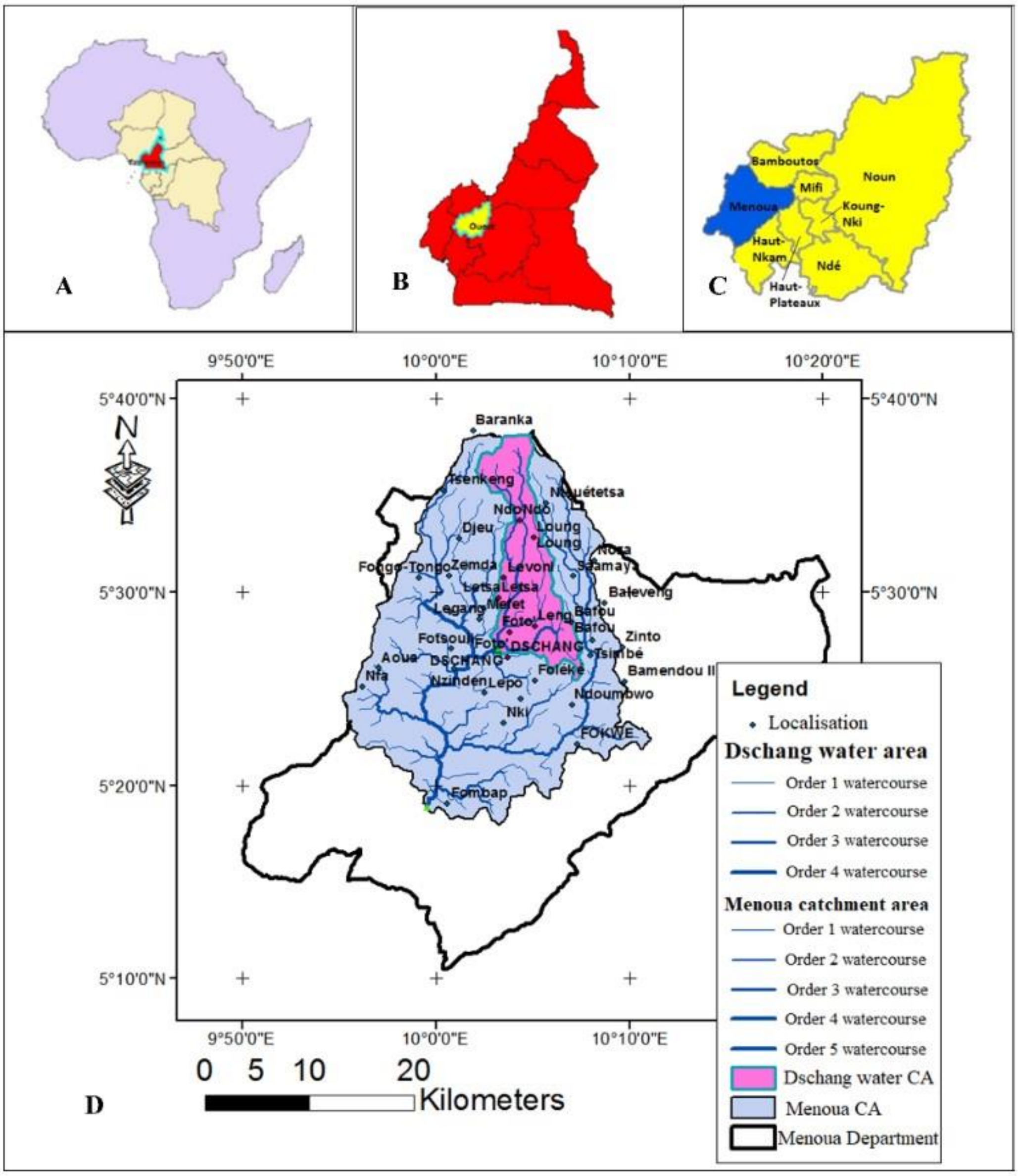

Figure 1. Location of the Menoua department **(D)** in the west **(C)** of Cameroon **(B)**, in central Africa **(A)**.

The assessment of the climatic vulnerability of the study area considers the parameters already proposed in the literature, i.e., exposure, sensitivity, potential impact, and adaptive capacity, in an aim to assign indices to each parameter to enable a more objective, quantitative assessment rather than a purely qualitative one. The first step is to analyze the parameters of climatic vulnerability and their influence on the agricultural calendar. The second step is to prioritize the various parameters in order to assign points and scores to them for the purpose of calculating the climatic vulnerability index.

2.2. Analysis of the parameters of the climate resilience

2.2.1. Exposure

The evaluation of exposure parameters uses standardized anomalies and trends, the determination of which is done respectively according to the formulas of Equations (1) and (2).

$$A_j = \frac{Y_X - \bar{Y}x}{\delta x} \quad (1)$$

In the correlation test, the null hypothesis H0 accepted here is that the classification of the variables is independent, and the variables are not correlated. The alternative hypothesis H1 accepted here is the data in the sample show a trend.

$$T = \frac{\text{agreeing} - \text{disagreeing}}{\sqrt{\text{agreeing} + \text{disagreeing} + \text{same X}\sqrt{\text{agreeing}} + \text{disagreeing} + \text{same Y}}} \quad (2)$$

The Sen slope according to the formula of Equation (3) consists of calculating the median of each pair of the time series with each measurement assigned to a regular interval.

$$B_{ij} = \frac{X_i - X_j}{i - j} \quad (3)$$

If the slope is statistically significant at the 95% threshold, then the result obtained is a robust estimate of the amplitude of the trend.

Identifying climate change using the Pettitt test according to the formula of Equation (4).

$$KN = max(t)\left|U1, N\right| \quad (4)$$

The $U1$, N statistic is considered for values of t bounded between 1 and N with KN the variable defined by Pettitt.

2.2.2. Sensitivity of systems to monthly rainfall distribution

Sensitivity is the degree to which the system is positively or negatively affected by exposure. Analysis of the monthly rainfall distribution will enable us to find consecutive accumulations of rainy days that give rise to the rainy season, implying the impact on cropping habits.

2.2.3. Potential impact

The combination of exposure and sensitivity determines the potential impact of climate change. The influence of fluctuations in the precipitation regime on water resources in the study area is assessed by measuring flows using the reel and identifying water-related illnesses or waterborne diseases diagnosed in patients in the study area during a survey.

The influence of fluctuations in the rainfall regime on water resources in the study area was assessed by measuring flow rates using a reel and identifying water-related diseases or waterborne illnesses diagnosed in 3555 patients in 7 health facilities in the study area during a survey.

2.2.4. Adaptation to climate change by people

The capacity of populations to adapt to climate variations and extremes to mitigate the negative effects and enhance the positive effects is assessed during field surveys/interviews. It depends on knowledge, technology, institutions and the economy. In this way, pollution indicators can be identified.

2.3. Assessing the climate vulnerability of the study area

The assessment of climate vulnerability using the AHP (Analytic Hierarchy Process, multi-criterion method, developed by Saaty in 1987) method is carried out in two stages.

The first stage is the identification (the parameters considered are those that can produce a damaging event and whose elements are known, even if the attributable values can be estimated according to their level of influence on the quality and quantity of the water), classification, and assignment of scores to climate vulnerability parameters according to **Table 1**.

Table 1. Rating scale [22].

Note	Importance level
1	Equal importance
3	Not very important
5	More important
7	Very important
9	Extremely important
2, 4, 6, 8	Intermediate importance

The comparison matrix of the different parameters by Saaty pair is presented as in **Table 2,** where *P* is the parameter identified and *n* is the number of parameters considered. ∑ai is the sum of the values in column *i*.

Table 2. Parameter comparison matrix skeleton.

	P_1	P_2	…	P_{n-1}	P_n
P_1	1	$X1$	…	X_{i-1}	X_i
P_2	$1/X1$	1	…	X_{i+2}	X_{i+3}
…	…	…	1	…	…
P_{n-1}	$1/X_{i-1}$	$1/X_{i+2}$		1	X_{i+4}
P_n	$1/X_i$	$1/X_{i+3}$		$1/X_{i+4}$	1
∑ai	∑column 1	∑column 2		∑column n−1	∑column *n*

After the binary combinations, we will check the consistency of the judgments (logical consistency) and then make the combinations to determine the weights.

The second and final stage is the determination of parameter weights and verification of logical consistency. The weighting coefficient (C_p) for each parameter corresponds to the intensity of its impact on the study of the vulnerability of life systems to climate variations. These coefficients are determined in two stages.

Step 1: Determining the eigenvectors (V_p) of each parameter according to the formula of Equation (5).

$$V_p = \sqrt[K]{w_1 \times w_2 \times \ldots \times w_k} \tag{5}$$

Step 2: Calculating the weighting coefficient (C_p) for each parameter according to Equation (6).

$$C_p = \frac{V_p}{\Sigma V_p} \tag{6}$$

With V_p the eigenvector of the parameter whose weighting coefficient C_p is to be calculated and $\sum V_p = V_{p1} + V_{p2} + \ldots + V_{pk}$ the different eigenvectors of each parameter. The sum of the weighting coefficients, C_p, of all the parameters in a matrix must be equal to 1.

The verification of the logical consistency or consistency ratio (RC) of the matrix uses Equation (7). If the value of the consistency ratio exceeds 10%, the assessments may need to be revised.

$$\mathrm{RC} = \frac{\mathrm{IC}}{\mathrm{IA}} \tag{7}$$

The values of the random index IA are given as a function of the number of parameters compared, and these values have already been determined by Saaty (**Table 3**).

Table 3. Random index based on the number of items compared [23].

Number of elements	**2**	**3**	**4**	**5**	**6**	**7**	**8**	**9**	**10**
Random Index **(**IA**)**	0	0.58	0.9	1.12	1.24	1.32	1.41	1.45	1.49

The consistency index IC is determined by the formula of Equation (8).

$$\mathrm{IC} = \frac{\lambda_{max} - Number\ of\ items\ compared(K)}{Number\ of\ items\ compared\ (K) - 1} \tag{8}$$

Determination of the rational priorities (λmax) using Equation (9).

$$\lambda_{max} = \frac{\mathrm{E}}{\mathrm{K}} \tag{9}$$

3. Results

3.1. Analysis of climate vulnerability parameters

3.1.1. Exposure

A) Normality test for climatic data (precipitation, temperature, and number of rainy days).

A good test of the normality of the climatic parameters considered requires these parameters to be characterized (**Tables 4** and **5**).

i) Normality test for southern zone climate data.

Table 4. Characteristics of the climate parameters collects at the IRAD rain gauge station.

	Year		**Average annual rainfall (mm)**		**Average annual temperature (℃)**		**Total rainy days**	
	Statistics	**Standard error**	**Statistics**	**Standard error**	**Statistics**	**Standard error**	**Statistics**	**Standard error**
Average	1997	1.948	9.347	0.278	19.513	0.344	163	6.249
Average truncated at 5%	1997		9.246		19.621		165	
Median	1997		9.162		20.692		175	
Standard deviation	12.923		1.846		2.150		32.473	
Minimum	1976		5.800		15.500		95	
Maximum	2020		14.800		21.600		205	
Asymmetry	0.020	0.357	0.889	0.357	−1.055	0.378	−0.963	0.448
Kurtosis	−1.172	0.702	1.388	0.702	−0.610	0.741	−0.384	0.872

Table 4 shows that the mean truncated at 5% is equal to the median for the years of the observation period and that the mean annual rainfall intensity is almost equal. These results show that among all the climate parameters considered (rainfall, temperature, and number of rainy days), only the distribution of years and the distribution of annual rainfall intensities show a distribution that could be normal and correlated. In addition, the coefficient of asymmetry for each of these two parameters is zero, indicating a centered grouping. The distribution according to the kurtosis coefficient of, firstly, the years tends to the right (−1.172) and, secondly, the mean annual rainfall intensity tends to the left (0.702). As for the average annual temperature and the total number of rainy days, the coefficient of asymmetry and the kurtosis coefficient are negative, evidence of dispersed distributions, and both (temperature and number of rainy days) tend towards the right.

The results of the normality test for rainfall, temperature, and number of rainy days in the southern part of the study area collected at the IRAD rain gauge station are shown in **Table 5**.

Table 5. Normality tests for data collect at the IRAD rain gauge station.

	Kolmogorov-Smirnov[a]			**Shapiro-Wilk**		
	Statistics	**ddl**	**Sig.**	**Statistics**	**ddl**	**Sig.**
Average annual rainfall	0.102	44	0.200*	0.952	44	0.067
Average annual temperature	0.276	39	0.000	0.746	39	0.000
Total rainy days	0.275	27	0.000	0.847	27	0.001

Notes: [a] Correcting the meaning of Lilliefors. * This is the lower limit of true significance.

Table 5 shows the significance of the normal distribution of the mean annual rainfall intensity data according to the Kolmogorov-Smirnov test, which follows the Lilliefors significance correction.

ii) Normality test for the data supplied by the sensors.

The normality test for the data supplied by the sensors is carried out separately from that of the data collected in the rain-gauge station because of the scale of the measurements, to minimize errors and discrepancies. The characteristics of the data supplied by the sensors are shown in **Table 6**.

Table 6. Characteristics of climate parameters provided by sensors.

	Year		**Average annual rainfall (mm)**		**Average annual temperature (℃)**		**Total rainy days**	
	Statistics	**Standard error**	**Statistics**	**Standard error**	**Statistics**	**Standard error**	**Statistics**	**Standard error**
Average	2002	1.76	2215.65	91.57	18.03	0.05	250.86	2.21
Average truncated at 5%	2002		2185.81		18.02		250.78	
Median	2002		2249.00		18.00		249.50	
Standard deviation	10.54		549.44		0.32		13.30	
Minimum	1985		1501.71		17.40		222	
Maximum	2020		3544.69		18.80		282	
Asymmetry	0.00	0.39	0.67	0.39	0.36	0.39	0.23	0.39
Kurtosis	−1.20	0.77	−0.10	0.77	−0.17	0.77	0.19	0.77

Table 6 shows equality between the standard mean, the mean truncated at 5%, and the median for the years of the observation period, followed by near equality for the mean annual temperature. These results show that among all the climate parameters considered for this study, as supplied by the sensors (year under consideration period, rainfall, temperature, and number of rainy days), only the distribution of the years under consideration period and the distribution of mean annual temperatures show a normal and potentially correlated distribution. In addition, the coefficient of asymmetry for each of these two parameters is zero, indicating a centered grouping. The distribution according to the kurtosis coefficient of the two parameters tends towards the right: Years (−1.20) and temperature (−0.17). As for the annual humidity values representing precipitation, the standard error of the mean is very high. However, the totals for the number of rainy days have an acceptable standard error of the mean but are not representative of the reality on the ground. This can be explained by the fact that the values attributed to rainfall are humidity values measured by the sensors according to atmospheric conditions; hence the good temperature values obtained.

However, the coefficient of asymmetry and the kurtosis coefficient for all the parameters considered show the same standard errors. The previous result could be proof that all the climate parameters supplied by the platform have the same errors and come from measurements by satellite sensors based on the displacement of cloud masses and magneto-telluric radiation from the Earth's geomagnetic fields. The hypothesis thus formulated admits a correction to be applied to the climatic parameters provided by the sensors in an intention to compensate for the lack of data usable by farmers due to the absence of a rain gauge station.

iii) Correction of discrepancies in data supplied by sensors.

In the case of this study, the data from the Agricultural Research Institute for Development station in Dschang, followed by observations of climatic phenomena in the field (rainfall and ambient temperature), were compared with the data values provided on the platform (rainfall and ambient temperature) with the aim of determining a correction procedure. The result of the correction procedure for the data supplied by the sensors and applicable to the South West flank of the Bambouto Mountains is as follows:

a) First, to obtain the rainy days, eliminate all precipitation values that are strictly lower than the value at which precipitation occurs in the field by replacing them with 0.
b) Then count as a rainy day the daily values greater than or equal to the reference value, which corresponds to the number 5 in the study area.
c) Finally, truncate the representative rainfall values by 5% using the following mathematical model: $Pi = 0.95P_0$; and for the extreme values, use the following mathematical model as a correction: $Pi = P0 - 5NJri$; $NJri$ being the total number of rainy days in the year I considered.

Following the application of this correction procedure, the new characteristics of the parameters studied are those shown in **Table 7**.

Table 7. Characteristics of the treated climate parameters provided by sensors.

	Year		**Average annual rainfall (mm)**		**Average annual temperature (°C)**		**Total rainy days**	
	Statistics	**Standard error**	**Statistics**	**Standard error**	**Statistics**	**Statistics**	**Standard error**	**Statistics**
Average	2002	1.76	1732.73	5.05	18.03	0.05	152	4.21
Average truncated at 5%	2002		1729.03		18.03		152	
Median	2002		1873.17		18.00		159	
Standard deviation	10.54		450.29		0.32		25.24	
Minimum	1985		1022.55		17.40		109	
Maximum	2020		2586.78		18.80		199	
Asymmetry	0.00	0.39	−0.12	0.39	0.36	0.39	−0.35	0.39
Kurtosis	−1.20	0.77	−1.14	0.77	−0.17	0.77	−0.93	0.77

Table 7 shows that the standard error on rainfall values has been considerably reduced. The total number of rainy days is acceptable and very close to reality in the study area.

The result of the normality test on the corrected data for rainfall, temperature, and number of rainy days in the northern part of the study area (Ndoh, Lekwué and surrounding areas) collected by the sensors is shown in **Table 8**.

Table 8. Normality test for data from the northern section.

	Kolmogorov-Smirnov[a]			**Shapiro-Wilk**		
	Statistics	**ddl**	**Sig.**	**Statistics**	**ddl**	**Sig.**
Year	0.068	36	0.200*	0.957	36	0.169
Average annual temperature	0.100	36	0.200*	0.979	36	0.696
Total rainy days	0.131	36	0.125	0.936	36	0.037
annual rainfall	0.137	36	0.087	0.942	36	0.057

Notes: *. This is the lower limit of true significance. [a]. Lilliefors meaning correction.

Table 8 shows the significance of the normal distribution of the mean annual temperature data and the distribution of the years of observation according to the Kolmogorov-Smirnov test, which follows the Lilliefors significance correction. The values for rainy days and rain intensities are not significant and therefore do not conform to the normal distribution.

B) Correlation test of climatic data (precipitation, temperature, and number of rainy days).

The correlation test is shown in **Tables 9** and **10**.

Table 9. Pearson correlations for data.

		Year	Average annual rainfall (mm)
Year	Pearson correlation	1	0.304*
	Sig. (bilateral)		0.044
	N	44	44
Average annual rainfall (mm)	Pearson correlation	0.304*	1
	Sig. (bilateral)	0.044	
	N	44	44

Note: *. The correlation is significant at the 0.05 level (two-tailed).

Table 9 shows that there is a significant correlation at the 5% level between the years of observation and the average annual rainfall. The rainfall intensity data for the different years, therefore, show an increasing trend in average intensity.

Table 10. Kendall's and Spearman's correlations of the data.

			Average annual temperature (°C)	Total rainy days
Kendall's Tau-B	Average temperature	Correlation coefficient	1.000	−0.396**
		Sig. (bilateral)		0.004
		N	39	27
	Total rainy days	Correlation coefficient	−0.396**	1.000
		Sig. (bilateral)	0.004	
		N	27	27
Spearman's Rho	Average temperature	Correlation coefficient	1.000	−0.572**
		Sig. (bilateral)		0.002
		N	39	27
	Total rainy days	Correlation coefficient	−0.572**	1.000
		Sig. (bilateral)	0.002	
		N	27	27

Note: **. The correlation is significant at the 0.01 level (two-tailed).

Table 10 shows that there is a significant correlation at the 1% level between the mean annual temperature and the total annual number of rainy days over the observation period. The temperature and rainy-day data therefore show a decreasing trend of undefined intensity, which would be due to random fluctuations in the various values observed.

The correlation test therefore reveals that in the Dschang and surrounding area, the intensity of rainfall varies from year to year, and the average annual ambient temperature is a function of the amount of rainfall during the year. Sunshine levels also vary according to the state of the atmosphere. However, in the area from Ndoh to Lekwué and its environs, the correlation test reveals that temperatures vary from year to year and the intensity of rainfall determines the duration of rainfall over the year.

C) Analysis of the climatic normal.

The diagram of average annual rainfall over the observation period (1966–2020) is shown in **Figure 2**. This diagram illustrates the fluctuation in cumulative annual rainfall over the observation period.

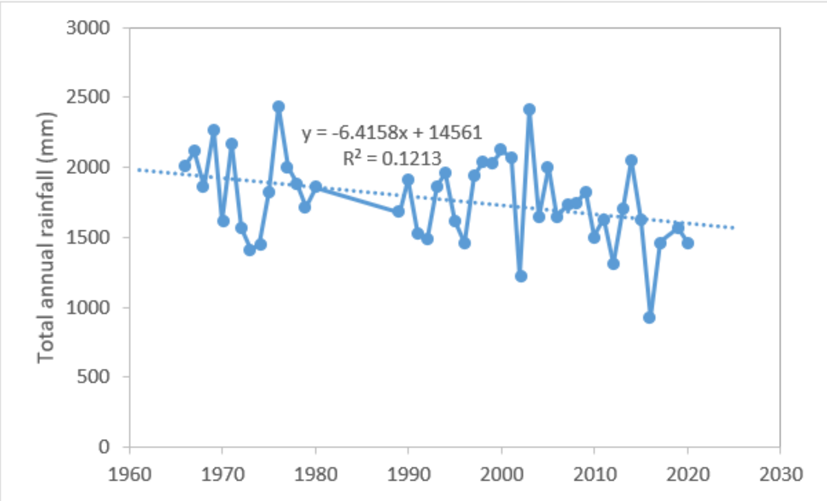

Figure 2. Diagram of cumulative annual rainfall over the observation period (1966 to 2020).

A data gap exists from 1981 to 1988. **Figure 2** shows that the rainfall series is broken down into relatively distinct rainfall regime periods. Cumulative rainfall over the whole of the study area follows a sawtooth pattern. Rainfall intensity follows the same sawtooth pattern, showing that some years are rainier than others. The distribution of rainfall in the study area is unimodal. The maximum value for cumulative annual rainfall in the south corresponds to 1976, with cumulative rainfall of 2431 mm. The minimum rainfall was in 2002, with a cumulative total of 1220 mm, corresponding to an average of 5.8 mm of rainfall per rainy day.

However, in the north zone, the wettest year was 2019, with a cumulative rainfall of 2059 mm, corresponding to an annual average of 15.3 mm of rain per rainfall event. The lowest rainfall was in 2013, when a total of 1206 mm of rainfall, corresponding to an average of 8.7 mm of rainfall. Climatic variability is therefore reflected in rainfall.

D) Normal analysis of the anomaly precipitation regime over the observation period (1976–2020).

The results reflecting the anomaly precipitation regime are derived from the interpretation of the rainfall anomaly diagram shown in **Figure 3**.

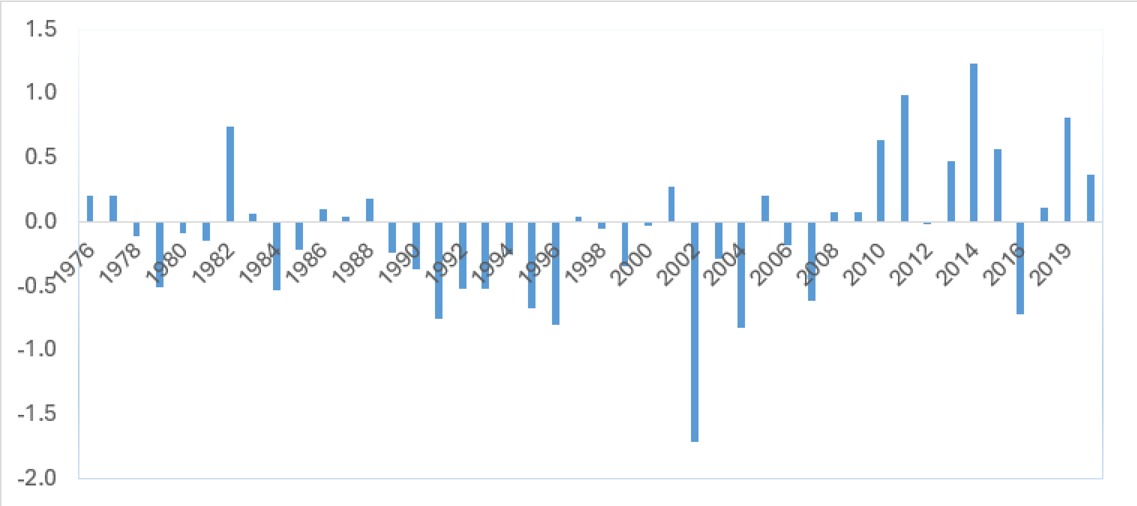

Figure 3. Diagram of annual rainfall anomalies over the observation period (1976–2020).

The rainfall anomaly diagram (**Figure 3**) shows the alternation of wet and dry phases over the observation period, reflecting the interannual change in rainfall anomalies in the Dschang zone and surrounding area. The maximum rainfall surplus was recorded in 2014, compared with a critical deficit in 2002. However, the northern zone recorded a maximum rainfall surplus in 2015, compared with a critical deficit in 2013.

This analysis of rainfall anomalies confirms that the average annual rainfall pattern has undergone changes over the observation period.

In the southern part of the Dschang water catchment area (the town of Dschang and the surrounding area), there was a dry decade from 1989 to 1999, followed by a rainy decade from 2008 to 2018. However, in the northern part (the area around Ndoh), a dry decade was recorded from 2004 to 2014, but no rainy decade was recorded during the observation period. These variations in seasonal distribution, such as the accentuated variation in rainfall, are at the root of disruptions to the agricultural calendar, resulting in increased or reduced yields. The homogeneity test (**Figure 4**) can be used to identify climate change in rainfall in the south of the country.

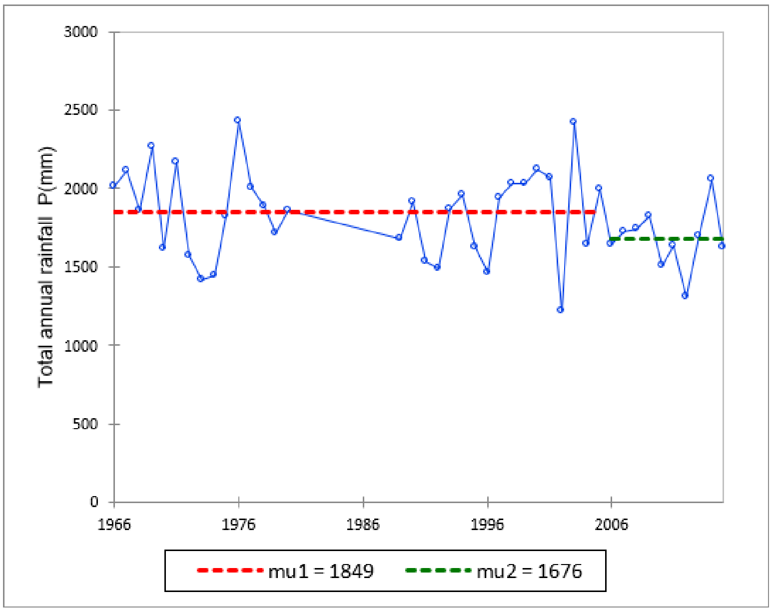

Figure 4. Test of the homogeneity of total precipitation over the observation period (1966 to 2020).

Figure 4 shows an average cumulative rainfall of 1849 mm between 1966 and 2005. Then an average cumulative rainfall of 1676 mm between 2005 and 2020. Variations in rainfall in the southern part of the study area have led to climate change in terms of precipitation from the break year 2005 onwards. The impact of this change is marked by a reduction in rainfall.

E) Normal analysis of rainy days over the observation period (1976–2020).

The curve showing changes in total rainy days over the observation period for the southern zone is presented in **Figure 5**.

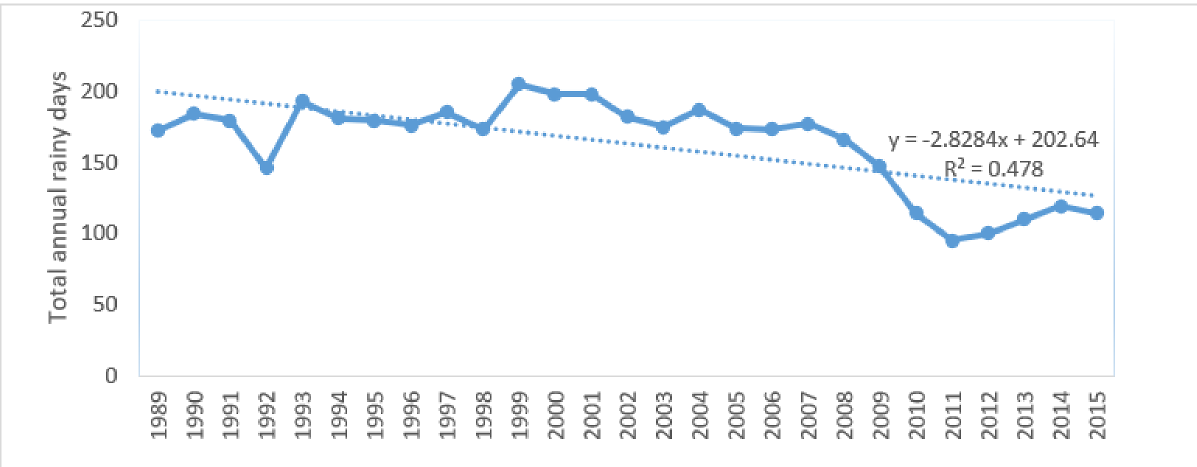

Figure 5. Variation curve of total annual rainfall days over the years.

Figure 5 shows that the maximum number of rainy days was reached in 1999, with 205 rainy days over the year, compared with a minimum of 95 rainy days in 2001. Since 2000, rainfall events and the number of rainy days have been falling. This decrease is justified by Sen's decreasing slope, with a negative regression coefficient of −2.8 calculated by extension over the entire observation period. The homogeneity test (**Figure 6**) identifies the climatic change in the number of rainy days.

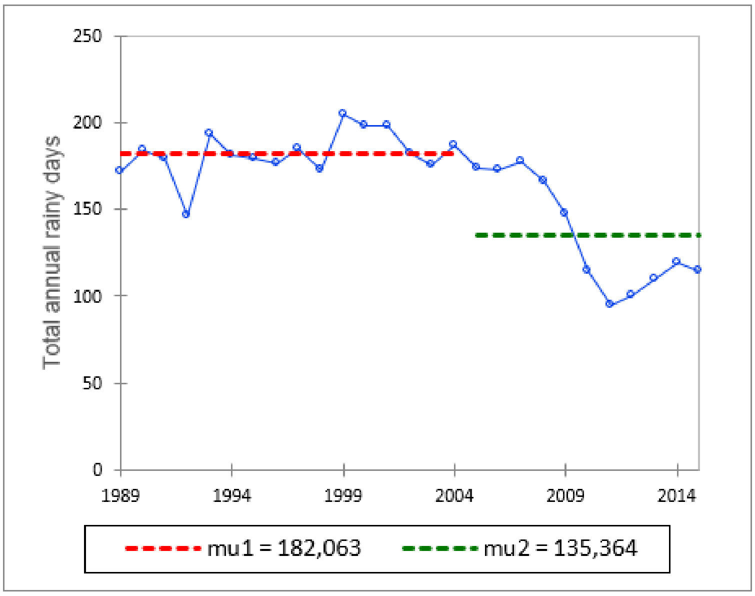

Figure 6. Test for the homogeneity of annual accumulated rainfall over the observation period (1989–2015).

Figure 6 shows an average cumulative annual rainfall of 182 days between 1989 and 2004. Then an average cumulative annual rainfall of 135 days between 2004 and 2015. Variations in the cumulative annual rainfall in the southern part of the study area led to climate change from the 2004-break year, which is close to 2005, the break year for cumulative rainfall.

F) Normal analysis of temperatures.

The variation curve for average annual temperatures over the observation period (1976–2020) for the study area is shown in **Figure 7**.

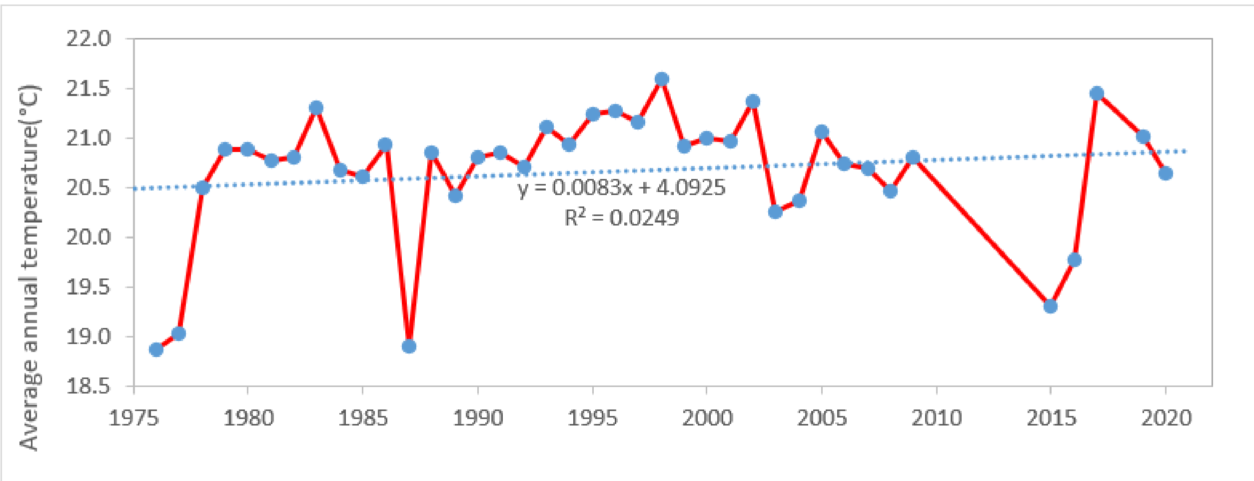

Figure 7. Average annual normal temperatures from 1976 to 2020.

The maximum temperature (**Figure 7**) was reached in 1998, with an average annual temperature of 21.6 °C, compared with lows of 18.9 °C in 1976 and 1987. Overall, over the observation period, temperatures have been rising at a slow rate.

The homogeneity test (**Figure 8**) makes it possible to identify climate change in terms of ambient temperatures.

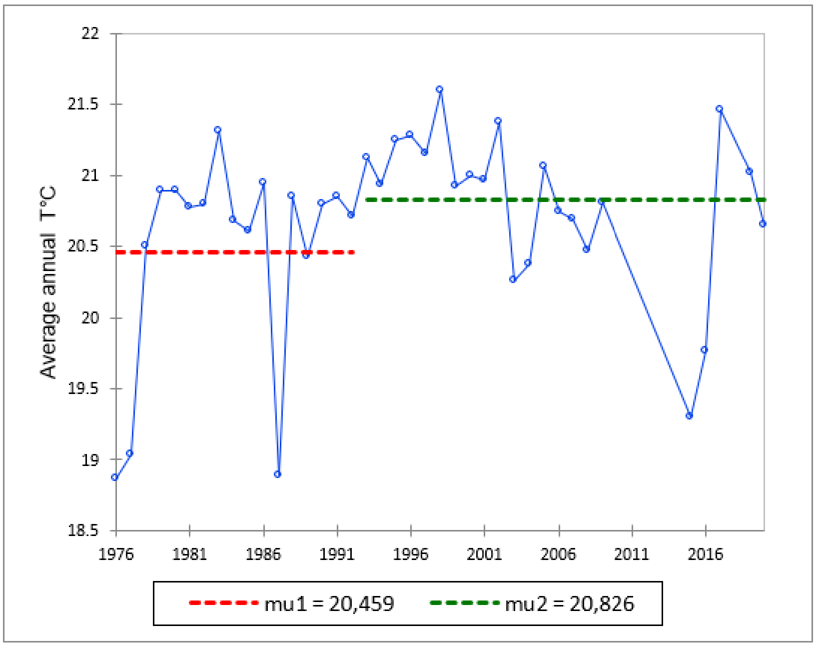

Figure 8. Test of the homogeneity of mean annual temperatures over the observation period (1976–2020).

Figure 8 shows an annual mean temperature of 20.5 °C between 1976 and 1992, followed by an annual mean temperature of 20.8 °C between 1992 and 2020. The increasing temperature variations in the southern part of the study area led to climate change from the break year 1992 onwards. Thus, the climate in the southern part of the study area has changed progressively, starting with ambient temperatures, which have increased by around +0.3 °C since 1992, followed by the number of rainy days, which has fallen by an average of around −47 rainy days since 2004, and finally, a fall in the amount of rainfall. This drop in the amount of rainfall is reflected in a reduction in the amount of rainfall of around −173 mm since 2005.

The annual average wet day calculated over the observation period in the southern zone is 163 days, and the number of consecutive rainy days varies spatially from 11 days. However, around 87 consecutive dry days are recorded. The average intensity per rainy day is 11.2 mm of rainfall, with a spatial distribution of three consecutive maximum rainy days estimated at 39.4 mm of rainfall. The cumulative total of 1613 mm represents the 90th percentile of rainfall. The number of rainy days above the 90th percentile is 4. So, the number of rainy days influences the amount of rainfall. However, the amount of rainfall and the frequency of rain events have no significant influence on temperature.

Analyses of the data provided by the sensors and then corrected on the basis of field measurements show that the climate in the northern part of the study area has changed gradually, starting with ambient temperatures, which have increased by around +0.4 °C since 1997; followed by the number of rainy days, which has fallen by an average of around −22 rainy days, again since 1997; and finally, the increase in rainfall of +630 mm between 2015 and 2020. This increase in rainfall in the summit zone of the southwestern slopes of the Bambouto Mountains would be favored by orographic rainfall in addition to frontal rainfall. The slight variation in ambient temperatures would be linked to the existing microclimates, created by the existence of waterfalls and cascades, not forgetting the effect of the high altitude (from 2400 m to 2723 m above sea level).

The annual average wet day calculated over the observation period in the north zone is 152 days, and the maximum number of consecutive rainy days is 17 days. However, around 103 consecutive dry days are recorded. The average intensity per rainy day is 11.4 mm of rainfall, with a spatial distribution of three days of maximum consecutive rainfall estimated at 40.4 mm of rainfall. The total of 2338 mm represents the 90th percentile of rainfall, equivalent to an average of 13.63. The number of days with rainfall above the 90th percentile was 9. The amount of rainfall and ambient temperature is therefore partly influenced by altitude, orography, and hydrography. Climate change is gradual, and its variation is spatiotemporal.

Exposure is the criterion directly linked to climatic parameters and necessary to determine the extent of climatic vulnerability. Typical exposure factors in the Dschang water catchment include: 1) Temperatures, which increase overall over the reference period; 2) the number of rainy events and rainy days, which decrease overall over the reference period; 3) rainfall, which increases with a shift in the annual peak rainfall intensity to either June, August, September, or October, marked by heavy rain. Extreme events are marked by heavy rain and strong winds.

3.1.2. Sensitivity

A) Impact of climate change on the agricultural calendar.

  i. Analysis of the monthly climate normal in the southern zone over the 1976-2020 reference period.

The exposure of the Dschang water catchment area to climate change leads to a degree of effect. The analysis of the monthly climate normal for the Dschang area and its surroundings over the reference period is shown in **Figure 9**.

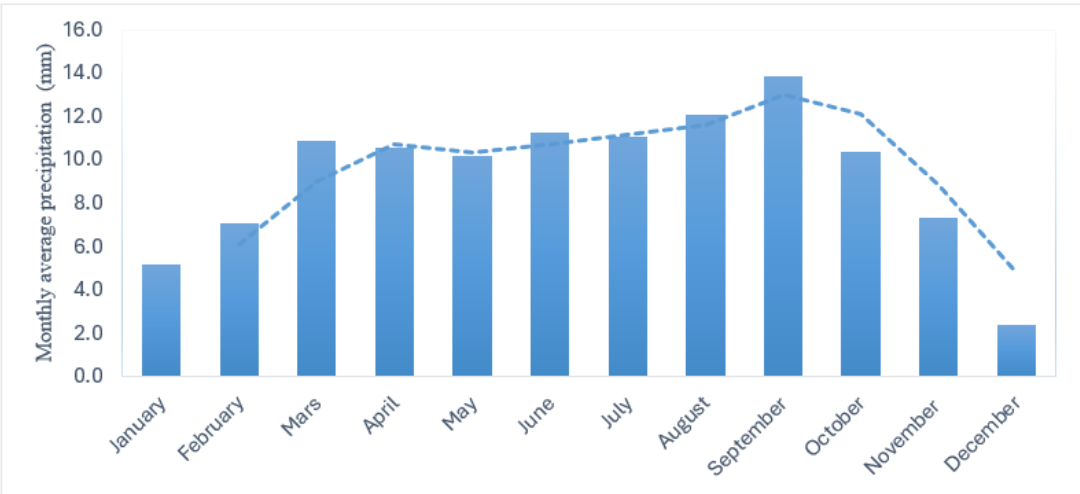

Figure 9. Average monthly rainfall from 1976 to 2020 in the southern zone.

The average monthly rainfall over the observation period is shown in the diagram in **Figure 9**. It is used to define the actual start of the rainy season to prevent farmers from continuing to lose seed following repeated sowing. The rainy season therefore begins in the southern zone when the cumulative rainfall on three consecutive rainy days is greater than or equal to 31.8 mm. Dry periods in this case must be less than 8 days with rainfall events of less than 10.6 mm. This minimum value falls within the calendar interval from 14 to 17 March and is what is needed to facilitate good ploughing and trigger the germination process. Rainfall peaks in September, the wettest month in the southern part of the study area. However, the driest month is December, a month marked by a sharp drop in rainfall between October and November until the rains disappear completely. The months of February and November form the backdrop to the wet period, although they make a small contribution to cumulative annual rainfall, with proportions of 1.7% and 2.7% respectively.

The dashed trend line in **Figure 9** shows an initial period of rapid recharge of surface water resources from February to mid-April. This is followed by a second, slower phase of recharge, coupled with a period when rainwater remains on the surface reservoirs between the end of April and the end of September. The discharge phase is rapid and occurs between the end of September and December, then from January to mid-February. This unimodal variation in rainfall cannot be compared with the bimodal variation in temperature.

The rise in temperature starts in January and stabilizes between March and April, while the second, smaller rise in temperature runs from August to October. Temperatures also fall in two phases: April to August and October to December. The minimum temperature is recorded in August.

ii. Analysis of the monthly climate normal in the northern zone over the reference period 1985–2020.

The analysis of the monthly climatic normal for the north zone (Ndoh area and its surroundings) over the reference period is presented by the curve and diagram in **Figure 10**.

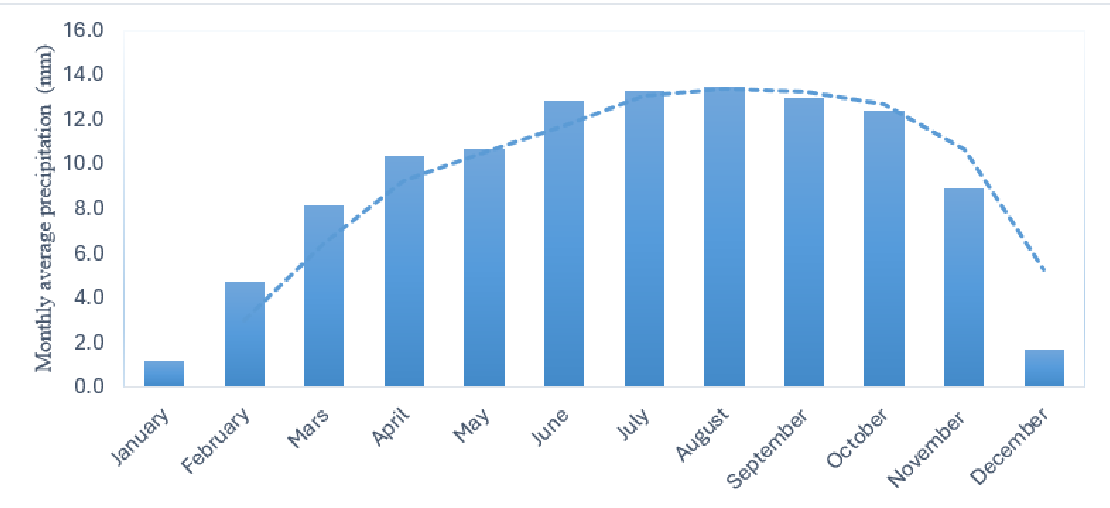

Figure 10. Average monthly rainfall for 1985–2020 in the northern zone.

The average monthly rainfall over 35 years is shown in the diagram in **Figure 10**. Rainfall peaks in August, which is the wettest month in the northern part of the study area. However, the driest month is January, which is marked by a sharp drop in rainfall between November and December until the rains disappear completely. The months of February and November form the backdrop to the wet period, although they make a small contribution to cumulative annual rainfall, with proportions of 0.6% and 2.8%, respectively.

The dashed trend line in **Figure 10** shows a period of rapid recharge of surface water resources from the end of February to the end of August. A second, slower phase of discharge occurs between September and the end of October. This discharge accelerates from November to December and then from January to February, when the river flows practically cancel each other out. The northern part of the study area therefore does not have a long residence time for rainwater in surface reservoirs. Surface water is then not available in sufficient quantity throughout the year to satisfy the demand for irrigation water from all farmers. This result is therefore evidence to justify the regular conflict over water for dry-season irrigation between farmers in the northern zone. The rainy season consequently begins when the cumulative rainfall on three consecutive days is greater than or equal to 33.4 mm. The dry sequences in this case must be less than 11 days with rainfall of less than 11.1 mm. This minimum value falls within the calendar period from 17 to 20 March and is what is needed to facilitate good ploughing and trigger germination processes in the northern zone.

The monthly temperature variation in the northern zone is unimodal. Temperatures rise in a single phase from August to December and then in January. The second phase is the drop in temperature, which begins in February and ends in August. The minimum temperature is recorded in August and the maximum in January.

Overall, over the study area, temperatures rise when precipitation falls. The average rise in temperatures and the fall of precipitation events directly affect the extent of the spatial and temporal distribution of surface water runoff. The variations in climate thus observed lead to climate change and have a direct influence on surface water resources.

The exposure of the Dschang water catchment to climate change leads to a degree of positive and/or negative affectation. In the case of positive exposure, the physical characteristics of the soil are resistant to erosion in the northern part (around Ndoh in the upstream part as far as Berinka). This resistance takes advantage of the soil cover following regular farming and the thickness of the HA horizon, which is around 70 cm thick with good porosity properties that favor good permeability. This is also the case for the A horizons, which are around 60 cm thick between Djuittitsa and Ndoh. Farming is therefore more widespread in this northern part of the study area. Plots where the cultivation method is to turn the soil over encourage rainwater infiltration.

The negative impact is more related to the characteristics of the natural environment. Winds are stronger at the summit, and bullying is more pronounced on steep slopes. The soils in the southern part (Dschang and the surrounding area), although well-drained and permeable, are still unstable. Runoff water is highly contaminated, with turbidity more than 4000 Nephelimetrical Turbidity Unit, reflecting the leaching of the soil. The slopes of the outlet are very steep, especially on the mountain range that forms the belt of the Foréké-Dschang escarpment. In addition to the above, cultivation methods involving the use of herbicides without turning over the soil encourage more intense run-off in agricultural plots. Water resources are subject to demographic pressure in densely populated areas. This demographic pressure, combined with a lack of civic-mindedness, leads to the emptying of rubbish bins and flush toilets into watercourses. As far as the hydraulic structures of boreholes and wells are concerned, these water supply structures are being over-exploited, hence the short period after the completion of these structures.

3.1.3. Potential impact of climate change

The impact of climate change on biosystems is the result of the combined effects of exposure and sensitivity.

A) Impact of climate change on the environment.

The impact of climate change as a result of the exposure of the Dschang water catchment area to heavy rainfall events, combined with the area's sensitivity due to its steep slopes and erosion-sensitive soils, resulted in a landslide with a mudflow on 4 August 2017 in Santchou; the destruction of 6 houses and the flooding of 185 households, followed by the collapse of the carriageway on the Dschang-Melong main road from 20 to 21 August 2020 in Santchou. A similar impact was observed on 1 September 2021 in the Toualé-Dschang district, where a landslide destroyed a house and flooding was observed in the Regie District.

B) Impact of climate change on agriculture.

The impact of climate change as a result of the Menoua's exposure to variations in heavy rainfall, combined with the area's sensitivity to variable soil properties, has resulted in variations in agricultural yields. Analysis of the impact of climate change on the crops most grown in the study area is shown in the curves in **Figure 11**.

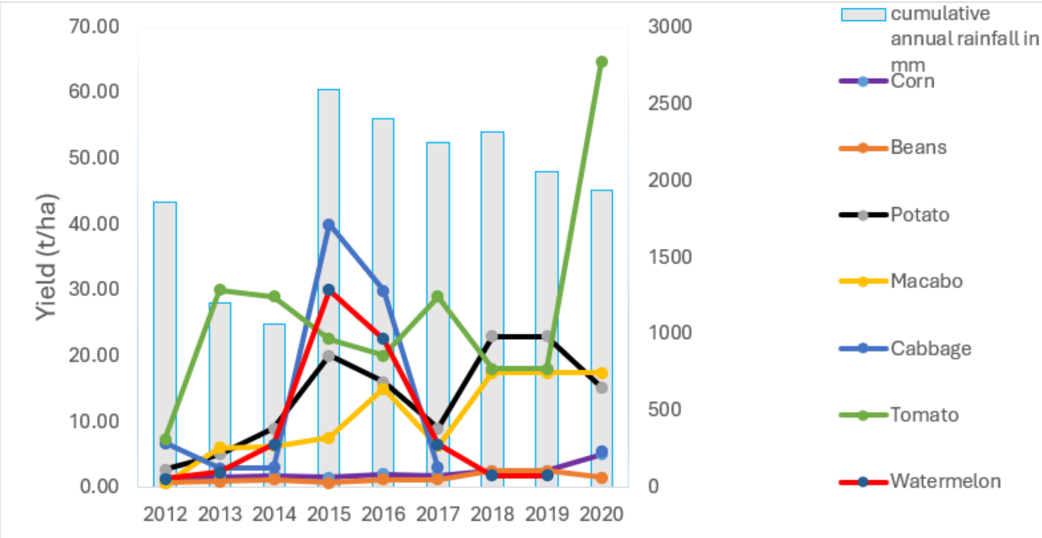

Figure 11. Annual yields of the most cultivated crops in Menoua department from 2012–2020.

Figure 11 shows that yields of cereals such as maize and beans are not influenced by annual variations in rainfall intensity. However, yields of tubers (macabo and potato) and vegetables (cabbage and tomato) are sensitive to rainfall variations. When annual rainfall intensity increases, yield also increases. Similarly, when rainfall falls, so does yield, except in the case of tomatoes, where the opposite is true. This has repercussions for farmers, who make up the largest proportion of the population in the Department of Menoua, with around 232,647 farmers out of a total population of 412,122 in 2020, i.e., 56.45% farmers.

C) Impact of climate change on surface water.

Most of the surface water in the Dschang water catchment comes from rainfall, and another proportion of groundwater support comes from springs and surface water/groundwater interaction in the drained valleys. **Figure 12** shows the diagram of annual variations in flow at the outlet of the Dschang water catchment as a function of rainfall.

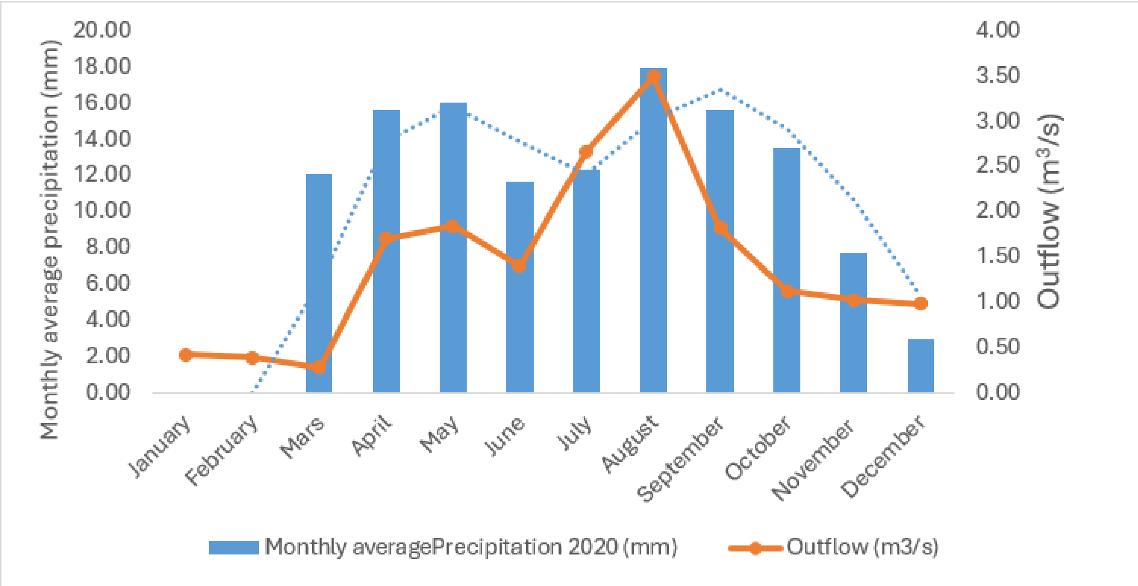

Figure 12. Rainfall-runoff diagram for 2020.

The dotted rainfall trend curve in **Figure 12** can be superimposed on the continuous flow curve. The flow of the outlet increases gradually between January and mid-August, then decreases between mid-August and the end of December. This variation in flow is superimposed on the variation in rainfall in the southern zone over the course of 2020. Faced with variations in rainfall, farmers put pressure on surface water to irrigate; it is this pressure that very often leads to conflicts between farmers upstream and downstream of watercourses, on the one hand, and between farmers and livestock breeders on the other.

D) Impact of climate change on groundwater.

Figure 13 is a diagram showing the movement of the water table in 2020 in relation to rainfall.

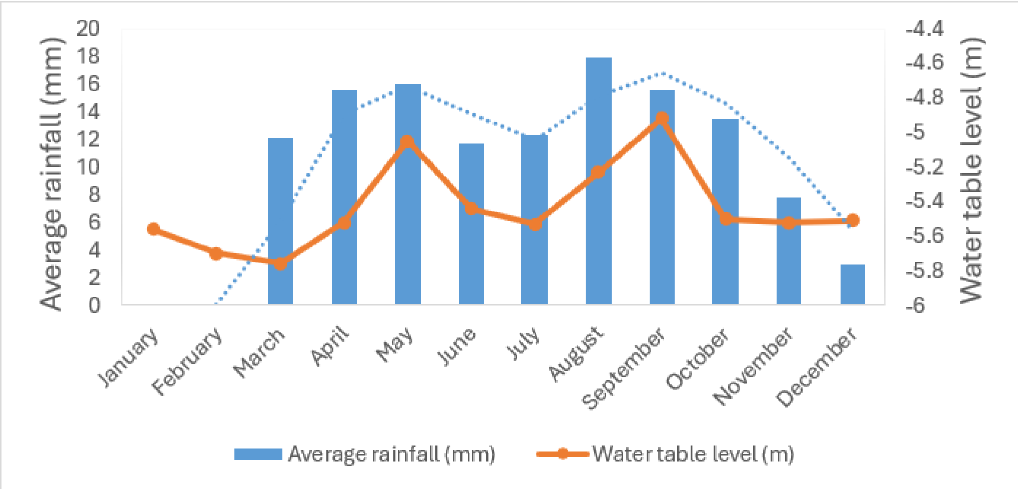

Figure 13. Rainfall-runoff diagram for the water table in 2020.

Figure 13 shows that the groundwater table in the subsurface aquifers fluctuates in line with rainfall, as the rainfall variation curve for 2020 is superimposed on the groundwater table fluctuation curve for 2020. The current consequences of this significant fluctuation in the water table in the field are a drop in the water level and the drying up of wells, an increase in the number of non-functional human-powered boreholes, and an increase in the demand for drinking water. Maximum recharge and critical discharge depend on rainfall patterns. Since people rely on rainwater, springs, streams and boreholes, the quality of life of people in the study area depends on the quality and availability of these alternative water supplies.

E) Influence of rainfall fluctuations on the quality of water resources in the study area.

The influence of the changes observed on the well-being of the population is assessed by surveys consisting of diagnosing water-related illnesses in 3555 individuals received in 7 health facilities during 2021 (**Figure 14**).

The survey results show that the population is more affected by water-related vector-borne diseases at a rate of 50% of total water-related diseases. The group of water-related vector-borne diseases in the study area is most represented by malaria, with a rate of 86.49%. This disease is most prevalent in April, September, and October, and least prevalent in February and May. The second is viral gastroenteritis with a rate of 12.01%, followed by filariasis at 0.7%, onchocerciasis at 0.5%, and yellow fever at 0.3%.

The second major group of water-related diseases affecting the population is the group of waterborne diseases caused by the consumption of poor-quality water. Water-borne diseases account for 44% of water-related illnesses. Typhoid fever is the most obvious disease in the group of communicable diseases following consumption of poor-quality water, with a rate of 69.1%. The second disease is bacterial gastroenteritis with a rate of 18.54%, followed by bacillary dysentery at 6.85%, then enteritis diarrhea at 5.39%, and finally cholera at 0.11%.

The third and final category of water-related illnesses recorded in the study area is that due to water scarcity. This group accounts for 6% of water-related diseases. The most common disease in this group is amoebiasis, which accounts for 65.52% of diseases caused by water scarcity. This is followed by dermatosis, which represents skin infections linked to the lack of water, with a rate of 25%, and finally ascariasis, with a rate of 9.48%. A representation of the rate of each group of diseases diagnosed in patients is shown in **Figure 14**.

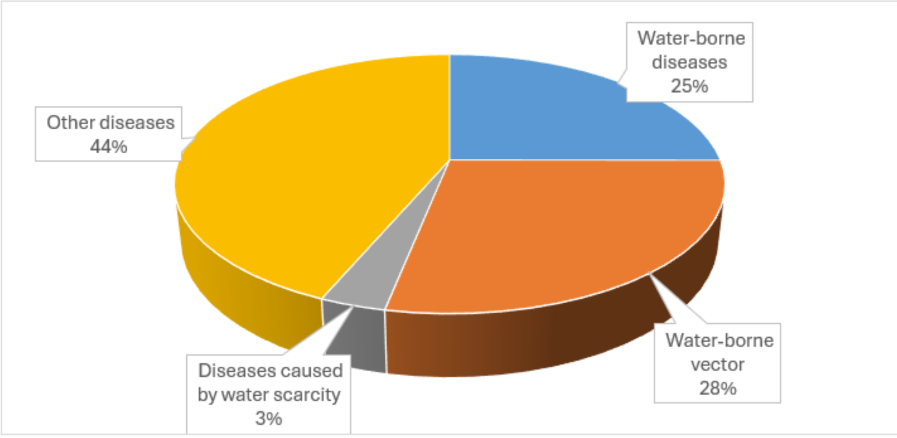

Figure 14. Proportion of diseases diagnosed in 2021.

Water-related illnesses account for the largest proportion, at 56%, compared with 44% for all other non-water-related illnesses.

3.1.4. Adaptation

Populations exposed to climate variations and extremes have developed the capacity to adapt to climate change to mitigate the negative effects and enhance the positive effects. In this way, they exploit the opportunities available to them to cope with the consequences of climate change. Adaptation takes place at four levels:

i) Knowledge, which occupies an acceptable position, as the populations of the study area are informed and aware of climate change and its effects;

ii) Technology, which considers the availability and accessibility of adaptive technologies; however, due to the lack of funding and financial resources among the majority of farmers, the absence of state subsidies, and the inadequate funding of decentralized state services, farmers are opting for improved seeds, fertilizers, animal excrement and phytosanitary products. Another adaptation measure is the improvement of existing technology through the homemade manufacture of turnstiles and the construction of mini earth dams to capture irrigation water; the creation of green spaces and reforestation in urban areas;

iii) Institutions, in terms of the legal institutional aspect and in relation to governance, facilitate the participatory approach to guarantee sustainable management of natural, financial, and human resources. To this end, the application of environmental laws, the transparency of procedures and decision-making are carried out on a daily basis by parasitical companies and organizations: MINADER, IRAD, COOP/GIC, Base phytosanitaire, Projet ACEFA, PIDMA, AFOP and many others;

iv) Economy: For the study area, the microeconomic level encompasses domestic sources of income (agriculture, services, trade, and small-scale livestock farming), housing and expenditure.

3.2. Assessment of the climatic vulnerability of Dschang water

3.2.1. Relational analysis of parameters

Observation of climate parameters (precipitation, temperature, number of rainy days) over the observation period shows a climate change that reflects the exposure of biosystems. If climate change is not observed (no break in the time series), exposure is of little significance. But if there is climate change, exposure is significant or very significant and causes effects that constitute impacts.

Sensitivity is low when exposure is low. Sensitivity defines the level of impact when it is medium or high, depending on whether exposure is high or very high. Exposure and sensitivity, therefore, define the level of impact.

The impact is low when sensitivity is low and exposure is low. But the impact is significant or very significant when sensitivity is medium or high and exposure is high. The level of impact determines the capacity of biosystems to adapt.

The ability to adapt is very high when the impact or potential impact is low. This capacity is high, medium, or low when the impact or potential impact is significant or very significant (**Figure 15**). The hierarchy of parameters according to the saaty scale after relational analysis is presented in **Table 11**.

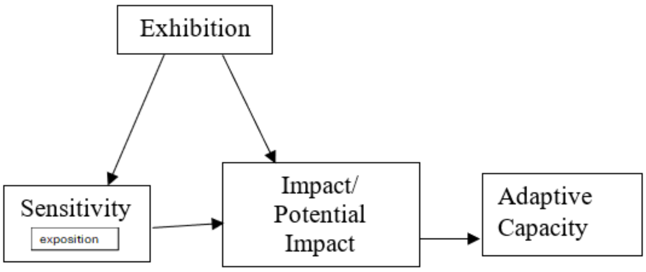

Figure 15. Relational analysis of parameters.

Table 11. Assigning notes to parameters.

Parameter	Gradation	Note
Exposure	Not important	3
	Important	4
Sensitivity	Low	3
	Medium	4
	High	5
Impact or potential impact	Low importance	3
	Important	6
	Very important	8
Adaptive Capacity	Low	8
	Medium	6
	High	4
	Very high	2

3.2.2. Weight determination

Binary combination

The scores considered in the original binary comparison matrix are those obtained when assigning the scores.

In **Table 12**, E is Exposure, S is Sensitivity, AC is Adaptive Capacity, and I is Impact and/or PI is Potential Impact.

Table 12. Original binary parameter comparison matrix.

Parameter	E	S	AC	I/PI
E	1	2	4	7
S	$\frac{1}{2}$	1	3	5
AC	$\frac{1}{4}$	$\frac{1}{3}$	1	3
I/PI	$\frac{1}{7}$	$\frac{1}{5}$	$\frac{1}{3}$	1
∑ai	1.89	3.53	8.33	16.00

Drawing up priority matrices and checking logical consistency

The priority matrix is used to determine the weights with the weighting coefficient (C_p). The logical consistency check validates the consistency of the original matrix, in which the parameters are ranked in ascending order of importance.

i. Priority matrix.

Table 13 shows that the weighting coefficient generally decreases. The climate vulnerability parameters are ranked in ascending order of impact on biosystems.

Table 13. Weighting of parameters.

Parameters	E	S	AC	I/PI	Eigen vector (V_p)	Weighting coefficient (C_p)	$C_p \times 100$
E	1	2	4	7	2.74	0.51	51
S	0.50	1	3	5	1.65	0.31	31
AC	0.25	0.33	1	3	0.71	0.13	13
I/PI	0.14	0.20	0.33	1	0.31	0.06	6
∑ai	1.89	3.53	8.33	16.00	5.41	1.00	100.00

ii. Verification of logical consistency.

The consistency ratio (**Table 14**) is less than 10% (CR = 1.2%) and therefore the original matrix is fine. **Table 15** summarizes the weights according to the scores used to calculate the climate vulnerability indices.

Table 14. Logical consistency matrix.

Parameters	E	S	AC	I/PI	Priority vector	Global priority	Rational priority	λ_{max}	Random index (IA)	Consistency index (IC)	Coherence ratio (RC)
E	0.53	0.57	0.48	0.44	0.50	2.04	4.06				
S	0.26	0.28	0.36	0.31	0.30	1.24	4.07				
AC	0.13	0.09	0.12	0.19	0.13	0.54	4.01	4.03	0.9	0.01	0.01
I/PI	0.08	0.06	0.04	0.06	0.06	0.23	4.00				
∑ai	1.00	1.00	1.00	1.00	1.00	4.05	16.13				

Table 15. Parameter weights and scores for calculating the climate vulnerability index.

Rating	E Exposure	S Sensitivity	AC Adaptive Capacity	I/PI Impact/potential impact
1 2 3	Low importance	Low	Very high	Low importance
4 5	Important	Medium	High	Important
6 7			Medium	Very important
8 9	Very important	High	Low	Extremely important
Weight	0.51	0.31	0.13	0.06

The climatic vulnerability index (Icv) = (0.51 CE) + (0.31 CS) + (0.13 CAC) + (0.06 CI).
where CE is the exposure rating, CS is the sensitivity rating, CAC is the rating corresponding to the ability to adapt, and CI is the impact or potential impact rating.

Applying the AHP method enables us to move from a qualitative assessment of climatic vulnerability to a quantitative assessment based on a robust ranking of the parameters according to the Saaty ranking scale. A summary of the weights and scores used to calculate the vulnerability index (used to represent the level of vulnerability) is shown in **Table 15**. Considering Saaty's rating scale and the results of the analysis of climatic vulnerability parameters for the Dschang water catchment, **Table 15** is used to rank the climatic vulnerability index (**Table 16**).

Table 16. Climate vulnerability index distribution.

Climate Vulnerability Index (Icv)	Degree of vulnerability
< 3	Low
3–5	Medium
5–7	High
> 7	Very high

Calculation of the vulnerability indices for the northern agricultural zone and the southern urban zone of Dschang water indicates two levels of climatic vulnerability: Low and medium. Low vulnerability has a vulnerability index of 1.89 in the summit zone (Lekwue), which is constantly covered by clouds, and on the mid-slope approaching the Bafou waterfall. In the greater part of the basin studied, vulnerability is generally moderate, but with vulnerability index values varying within the same range. The average climatic vulnerability index is 3.61 in the northern agricultural zone and 4.55 in the southern zone, corresponding to peri-urban and urban areas (**Figure 16**).

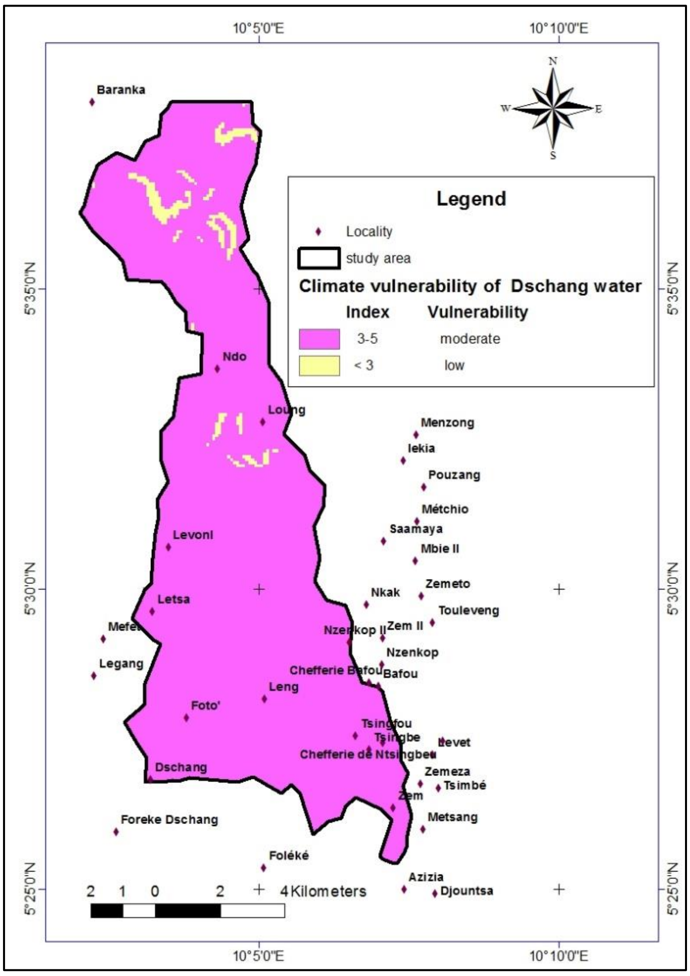

Figure 16. Climate vulnerability map in Dschang water catchment area.

The difference in climatic vulnerability index values is thought to be linked to the action of vegetation in the agricultural zone, coupled with altitude. Farming is intensive and involves a mixture of crops, with small crops mulching the soil. Agriculture would therefore be the practice that softens the climate by reducing the sensitivity of biosystems and thus reducing the potential impact of climate change. However, the new farming practices that use agricultural inputs to help adapt to climate change, as a result of soil impoverishment, produce pollutant loads. Physical pollutants are waste from residues and packaging of poorly managed plant protection products and chemical fertilizers. Chemical and microbiological pollutants are nitrogen derivatives, chlorine and phosphate derivatives and micro-organisms from livestock droppings that end up in the water consumed by the rural population. The various pollutants also travel southwards into the urban area. The study of specific potential pollutants will be the subject of future work in an aim to take them into account when assessing the specific vulnerability of water resources.

4. Discussion

Spatial and temporal variations in rainfall along the south-western slopes of the Bambouto Mountains are thus influenced by orography coupled with frontal rainfall resulting from climate change, which impacts water resources, agricultural production and the health of populations [4,6,8]. The uneven distribution of rainfall and temperatures has led to extreme events such as heavy rains and periods of atmospheric drought. Maximum rainfall in Dschang was 2053 mm in 2014 and 2059 mm in 2019 in Ndoh, compared with minimums of 1220 mm in Dschang in 2002 and 1206 mm in 2013 in Ndoh. Rainfall and temperature are subject to spatial and temporal variation, as recognized by [24–26].

Climatic variations in the study area have gradually led to climate change. This change is marked by the fall in rainfall, which began in 2005 with rainfall dropping from 1849 to 1676 mm. The number of rainy days also fell from 182 to 135 in 2005. However, the average annual ambient temperature has risen from 20.5 ℃ to 20.8 ℃ since 1992. In general, over a longer observation period (1966–2020) in Dschang, rainfall tends to decrease, with a break around 2005. Similarly, the number of rainy days is falling, and only the ambient temperature is tending to rise slightly. This result differs from that of [20], which states that in general, except for Dschang, where rainfall amounts are gradually increasing, the localities of Bafoussam and Koundja are experiencing a decrease in rainfall over the series studied (1970–2009). However, in the period studied by Amougou and colleagues, rainfall began to increase again from 1989 until 2003, before falling again. The increase in average temperatures proposed by these authors is of the order of 1.56 ℃ over the period as a whole, but this value is well above that for the study area. However, all the authors agree on the probable sowing periods, i.e., March and April, which are potentially the months when maize is sown.

The general decline in rainfall observed from 2004–2020 in Dschang is contrary to the forecasts of the United Nations Development Program [27] and Climate Services Center [28] global models, whose forecasts indicate a slight increase in perceptible rainfall amounts between 2010 and 2035. These forecasts also show a drop in rainfall amounts between 2075 and 2090, with fluctuating phases from one decade to the next. The consequences are felt on surface and subsurface water resources, river flow regimes, and environmental and economic resources. These results are in line with those of [29] on the development and analysis of vulnerability criteria for Sahelian populations faced with climate vulnerability. The increase in temperature and decrease in rainfall are in line with the global forecasts of the UNFCCC [30] and the IPCC [28], but the temperature increases coefficients and rainfall decrease coefficients found in this study are different from theirs. The differences are undoubtedly due to the fact that this study goes beyond the global framework and takes place on a much smaller scale. The increase in temperature in the study area remains low overall. These values are linked to the microclimate created by frontal and/orographic rainfall in the study area. These values could rise to between 2 ℃ and 5 ℃ by 2100 if nothing is done in Africa, which seems to be the region most affected by climate change. The results demonstrate the vulnerability of local populations to climate change, which affects most of the productive sectors of the socio-economic fabric.

The sensitivity of biosystems to observed changes in the climate, producing felt consequences on the surface and subsurface water resources, river flow regimes and environmental and economic resources, is widespread in the intertropical zone, according to the work of Bosson et al. [31]. According to [29], these sensitivities are among the criteria for vulnerability of Sahelian populations to climate vulnerability.

The decline in soil fertility is also linked to climate change, as recognized by Västilä et al. [32]. The population of the study area is adapting to climate change using precarious methods that are palliative to the world's high technology. Yet the country has a wealth of potential and natural resources that have so far been poorly exploited. The solution therefore lies in finding the best techniques for adapting to climate change [33,34], which are tailored to the realities of the populations concerned and take account of the cultures and customs of each person. Since good adaptation to climate change leads to a reduction in vulnerability to climate change. Such a feat can only be achieved with greater involvement from the state and its development partners.

The impact on water resources and on the economy is leading populations experiencing rapid demographic growth to seek alternative sources of water supply, the quality of which remains questionable [19,35,36]. An effort has been made to decentralize the management of drinking water supply and sanitation to decentralized local authorities. According to Temgoua et al., Santsa et al. the rate of water-related illness was 77% between 1999 and 2003 [37]. However, the efforts made by public authorities at local level are reflected in the rate of waterborne disease, which has fallen from 77% as mentioned above to 56% as revealed by the results of diagnoses carried out on the population of the study area following a socio-economic and health survey carried out in 2021.

Climate vulnerability is a concept that reflects the complex interaction between several factors that determine the sensitivity of the system. By quantifying the parameters of climatic vulnerability using the parameter hierarchy scale proposed by Saarti, it is possible to carry out a quantitative assessment by indexing the parameters using the AHP method.

5. Conclusion

The aim of this article was to examine climatic vulnerability in the humid tropics by indexing the parameters of exposure and sensitivity of biosystems to climate change to identify the new favorable sowing period. The impacts and capacity to adapt were then exploited to find clues that could guide future research into assessing the specific vulnerability of water resources, considering specific pollutants. The results show that the change is felt in rainfall from 2005 onwards, which marks the breakthrough year, with cumulative annual rainfall falling from 1849 mm to 1676 mm. The total annual number of rainy days fell from 182 to 135 in 2004, the breakthrough year. The average annual temperature, on the other hand, rose from 20.5 ℃ to 20.8 ℃ in the year 1992. This gradual change in climate has affected agro-pastoral activities, in particular by shifting the mid-point of the agricultural calendar from the beginning of March to the second third of the same month. Surface and groundwater have been adversely affected. As a result, 56% of the population suffers from water-related diseases. Adaptation measures include the use of improved seeds, organo-mineral and chemical fertilizers, pesticides, fungicides and slurry, the uncontrolled use of which results in the production of waste that causes pollution. The pollutants sought may therefore be physical, chemical (chlorine, nitrogen and phosphate by-products and heavy metals), and microbiological (fungi, molds and fecal contaminants). Indexing and ranking the various climatic vulnerability parameters reveals two levels of vulnerability: Low and medium. The need for States to take a particular interest in the climate is becoming apparent to boost and improve socio-economic development, which necessarily requires the ability to adapt to the realities of local populations.

Author contributions: Conceptualization, FFM and MCMM; methodology, FFM; software, RNN; validation, HGD, MCMM and ET; formal analysis, ET; investigation, FFM; resources, MCMM; data curation, RNN; writing—original draft preparation, FFM; writing—review and editing, HGD; visualization, MCMM; supervision, ET; project administration, ET; funding acquisition, FFM. All authors have read and agreed to the published version of the manuscript.

Conflict of interest: The author declares no conflict of interest.

References

1. Mba FF, Temgoua E, Kanouo BMD, et al. Assessment of the sensitivity of water resources in the intertropical zone: A bibliographical study with perspectives. Journal of Water Supply. 2023; 23(5): 19. doi: 10.2166/ws.2023.099
2. ADBG. Central African Economic Outlook. ADBG; 2018. p. 42.
3. AGW-Net. Integrating groundwater management for transboundary basin organisations in Africa. AGW-Net; 2015. p. 20.
4. Dettinger M, Udall B, Geory A. Western water and climate change. Ecological Applications. 2015; 25(8): 2069–2093.
5. Mubeen M, Ahmad A, Hammad HM, et al. Evaluating the climate change impact on water use efficiently of cotton-wheat in semi-arid conditions using DSSAT model. Journal of Water and Climate Change. 2020; 1661–1675.
6. You X, Li Z, Yi Y. Carbon constraints, industrial structure upgrading, and green total factor productivity: An empirical study based on the Yangtze River Economic Belt. Journal of Water and Climate Change. 2023; 14(9): 1–17. doi: 10.2166/wcc.2023.051
7. GIZ. Reference guide on vulnerability, concept and guidelines for conducting standardized vulnerability analyses (French). GIZ; 2017. p. 180.
8. Haward G, Charles K, Pond K, et al. Securing 2020 vision for 2030: Climate change and ensuring resilience in water and sanitation services. Journal of Water and Climate Change. 2010; 15.
9. UN-HABITAT. Time to think urban. UN-HABITAT; 2013. p. 32.
10. Jelani J, Mahdzir MMFM, Sabri WMSWM, et al. Determination of groundwater potential zone using geospatial and geophysical method for UPNM campus, Kuala Lumpur, Malaysia. Journal of Water Resources Management. 2024; 2(1): 1–7.
11. Nepal S, Shrestha AB. Impact of climate change on the hydrological regime of the indus, Ganges and Brahmaputra river basins: A review of literature. International Journal of Water Resources Development. 2015; 31(2): 201–218. doi: 10.1080/07900627.2015.1030494
12. Kushwaha P, Pandey VK, Kumar P, et al. Projection of mean and extreme precipitation and air temperature over India: a CMIP6 analysis. Journal of Water and Climate Change. 2024; 6(15): 2562–2581. doi: 10.2166/wcc.2024.523
13. Sonali P, Nagesh Kumar D. Review of recent advances in climate change detection and attribution studies: A large scale hydroclimatological perspective. Journal of Water and Climate Change. 2020; 1–29.
14. Güven A, Vedat M, Pala A. Modeling and future projection of streamflow and sediment yield in a sub-basin of Euphrates river under the effect of climate change. Journal of Water and Climate Change. 2024; 6(15): 2628–2647. doi: 10.2166/wcc.2024.612
15. Goodarzi MR, Abedi MJ, Niazkar M. Effects of climate change on streamflow in the Dez basin of Iran using the IHACRES model based on the CMIP6 model. Journal of Water and Climate Change. 2024; 6(15): 2595–2611. doi: 10.2166/wcc.2024.571
16. Enayati B, Bozorg-Haddad O, Bazrafshan J, et al. Bias correction capabilities of quantile mapping methods for rainfall and temperature variables. Journal of Water and Climate Change. 2021; 401–419.
17. Keskinen M, Chinvanno S, Kummu M, et al. Climate change and water resources in the lower Mekong river basin: Putting adaptation into the context. Journal of Water and Climate Change. 2010; 103–117.

18. WHO, UNICEF. Joint monitoring program for water supply and sanitation (JMP): progress on sanitation and drinking water. 2015. P. 15. Available online: https://www.unwater.org/publications/who/unicef-joint-monitoring-program-water-supply-and-sanitation-jmp-2015-update (accessed on 10 October 2024).
19. Mba FF, Temgoua E, Kengne PD, et al. Vulnerability of groundwater to pollution in the town of Dschang, West Cameroon (French). Int. J. Biol. Chem. Sci. 2019; 13(5): 39–56.
20. Amougou JA, Forghab Mbomba P, Batha RAS, et al. Rainfall and temperature in the West Cameroon region: Analysis of trends from 1950 to 2015 and projections to 2090 (French). ONACC; 2019. p. 148.
21. Temgoua E, Meli MV, Mekui M, et al. The role of decentralized local authorities in sustaining water and sanitation services in non-concession areas: The case of the Commune of Dschang. Int. J. Biol. Chem. Sci. 2019; 13(5): 122–132.
22. Saaty TL. The analytic hierarchy process: Planning priority setting, Resource allocation. MC Graw-Hill; 1980. p. 19.
23. Saaty TL. A scaling method for priorities in hierarchical structure. Journal of Mathematical Psychology. 1987; 15: 234–281.
24. Kengni L, Tekoudjou H, Tematio P, et al. Rainfall variability along the Southern flank of the Bambouto mountain (West-Cameroon). Journal of the Cameroon Academy of Sciences. 2008; 8(1): 45–52.
25. Kengni L, Simo PJ, Temgoua E, et al. Hydrogeochemical processes in the Southern slope of the Bambouto-Mountain (West-Cameroon). International Journal of Engineering Science and Technology. 2013; 5(4): 896–908.
26. Tazen F, Fonteh FM, Karambiri H. Integrated water resource management in the catchment area of the Dschang municipal lake: Knowledge and use. J. Biol. Chem. Sci. 2013; 7(2): 840–851.
27. McSweeney C, New M, Lizanco G. UNDP Climate Change Country Profiles. UNDP; 2008. p. 65.
28. CSC. 2013. Climate change scenarios for the Congo Basin. Climate Service Center; 2013. p. 165.
29. Mara F. Development and analysis of vulnerability criteria for Sahelian populations faced with climate vulnerability, the case of water resources in the Sirba valley in Burkina Faso (French) [PhD thesis]. Université du Québec à Montréal; 2010.
30. UNFCCC. Framework Convention on Climate Change: Project on activities carried out to implement the capacity-building framework in accordance with decision 2/CP.7. United Nations; 2006. p. 16.
31. Bosson F, Yira Y, Dayamba DS, et al. Mainstreaming climate change into water policies: A case study from Burkina Faso. Journal of Water and Climate Change. 2021; 1487–1500.
32. Västilä K, Kummu M, Sangmanee C, et al. Modelling climate change impacts on the flood pilse in the lower Mekong floodplains. Journal of Water and Climate Change. 2010; 67–86.
33. IPCC. Climate Change 2013: the physical science basis; Summary for policymakers, technical summary and frequently asked questions. United Nations; 2013. p. 222.
34. IPCC. Climate Change 2007: Synthesis Report. Intergovernmental Panel on Climate Change; 2007. p. 214.
35. Earman S, Dettinger M. Potential impact of climate change on groundwater resources: A global review. Journal of Water and Climate Change. 2021; 213–229.
36. Temgoua E, Santiago H, Pfeifer HR. Bacteriological pollution of groundwater and soil by nearby latrines in poor urban areas: the case of the city of Dschang. International Journal of Advanced Studies and Research in Africa. 2010; 228-242.
37. Santsa NCV, Ndjouenkeu R, Ngassoum MB. Water quality in Dschang and impact on consumer health. Afrique Science. 2018; 14(3): 96–107.